Available online at www.sciencedirect.com

ScienceDirect

Ceramics International 39 (2013) 9605–9611

CERAMICS INTERNATIONAL

www.elsevier.com/locate/ceramint

Fabrication and characterization of $Ba(Zr_{0.84}Y_{0.15}Cu_{0.01})O_{3-\delta}$ electrolyte-based protonic ceramic fuel cells

Sung Min Choi[a,b], Jong-Heun Lee[b], Ho Il Ji[a], Kyung Joong Yoon[a], Ji-Won Son[a], Byung-Kook Kim[a], Hae June Je[a], Hae-Weon Lee[a], Jong-Ho Lee[a,*]

[a]*High-Temperature Energy Materials Center, KIST, Seoul 136-791, Korea*
[b]*Department of Materials Science & Engineering, Korea University, Seoul, Korea*

Received 17 March 2013; received in revised form 13 May 2013; accepted 20 May 2013
Available online 4 June 2013

Abstract

Protonic ceramic fuel cells (PCFCs) were successfully fabricated by using 15 mol% Y-doped $BaZrO_3$-based electrolytes that have fairly good electrical conductivity and chemical stability. In order to overcome the poor sinterability of the $BaZrO_3$-based electrolytes, which is a critical limitation in making a thin-film electrolyte for electrode-supported PCFCs, we utilized sintering aid-assisted enhanced sintering by adding 1 mol % of CuO, thereby reducing the sintering temperature of the constrained thin electrolyte on a rigid electrode substrate to below 1500 °C. From the process optimization of the thin BZYCu coating on the NiO–BZYCu anode substrate, we fabricated a 10-μm-thick thin and dense electrolyte layer that exhibited an open-circuit voltage (OCV) close to that of the theoretical OCV of 0.98 V. However, improving the electrochemical performance by optimizing the electrode microstructure, especially in terms of the electrochemical activity of the anode and the current-collecting efficiency of the cathode, is the major concern of forthcoming study.

Keywords: E. Fuel cells; Proton conductor; Thin electrolyte; Sintering additive; $BaZrO_3$

1. Introduction

In order to solve the problem of exhaustion of fossil fuel energy resources and the environmental concerns raised from the use of fossil fuel energy, there has been a significant effort to utilize clean and renewable energy sources. Fuel cells are one of the most promising alternative energy generation systems used to substitute for conventional fossil fuel-based systems. Among various types of fuel cells, solid oxide fuel cells (SOFCs) have many advantages such as high energy efficiency, modularity, and high powder density [1]. However, SOFCs generally require high operating temperatures because the yttrium-stabilized zirconia (YSZ) electrolyte that is most frequently used shows reasonable ionic conductivity only at high temperatures above 800 °C [1–3]. Hence, many technical problems such as the poor stability of the thermomechanical and thermochemical properties of SOFCs have arisen due to these high operating temperatures [2,3]. In order to reduce the operating temperature of SOFCs, the development of alternative electrolytes has been pursued by many researchers [4–6]. Recently, proton-conducting oxides have been introduced as a new candidate material to replace conventional oxygen-conducting-based electrolytes such as YSZ and gadolinium-doped ceria (GDC) [7,8]. The use of a proton conductor as an electrolyte for SOFCs (Protonic ceramic fuel cells: PCFCs) results in high ionic conductivity and lower activation energy in the intermediate temperature range, thus reducing the cell operating temperature to below 500 °C [9].

Among the various proton conductors available, Ba-based perovskite-structured materials such as $BaZrO_3$ and $BaCeO_3$ doped by selected rare earth elements have been intensively investigated because of their high proton conductivities [10–13]. It is generally known that the bulk proton conductivity and chemical stability of $BaZrO_3$ are higher than those of $BaCeO_3$ in the intermediate temperature range of 500–700 °C. However, the apparent

*Corresponding author. Tel.: +82 29585532.
E-mail address: jongho@kist.re.kr (J.H. Lee).

0272-8842/$ - see front matter © 2013 Elsevier Ltd and Techna Group S.r.l. All rights reserved.
http://dx.doi.org/10.1016/j.ceramint.2013.05.081

conductivity of conventional polycrystalline $BaZrO_3$ is normally lower than that of $BaCeO_3$ because the grain boundary conductivity of $BaZrO_3$ is significantly lower than that of $BaCeO_3$ [12].

Acceptor doping can enhance the proton conductivity by generating oxygen vacancies that can be a source for the incorporation of water into the perovskite structure [14]. Among the various acceptor dopants, yttrium is the most effective one for $BaZrO_3$ because it exhibits good proton conductivity and low activation energy for migration in wide temperature ranges. However, Y-doped $BaZrO_3$ (BZY) is known to have a very refractive nature, and thus, it is very difficult to sinter. Temperatures of at least 1700 °C are needed in order to obtain 95% density. In order to practically apply BZY as an electrolyte material in intermediate temperature (IT)-SOFCs, this poor sinterability needs to be overcome [15]. Recently, it was reported that dense BZY could be obtained at a sintering temperature of 1500 °C by the addition of CuO and at 1300 °C by the addition of ZnO as sintering aids [13,15,16]. However, the formation of a thin-film BZY electrolyte on a rigid substrate is challenging compared with BZY bulk fabrication. Process flaws in the thin-film electrolytes on the electrode substrate are generally unavoidable because of the substrate constraint of bi-axial nature. [17]. Because the constrained sintering of thin films leads to restricted shrinkage in the lateral direction [18,19], thin electrolytes are always vulnerable to electrolyte leakage due to the development of structural defects in the direction normal to the substrate.

Here, we report the low-temperature fabrication of a thin, dense electrolyte based on 15 mol% Y-doped $BaZrO_3$, which is known to have extremely poor sinterability. To overcome this limitation, the thin BZY electrolyte on the NiO–BZYCu anode substrate was fabricated by using an enhanced sintering method with 1 mol% CuO as a sintering additive. In this study, the effect of the sintering additive on the microstructure of the electrolyte and the consequent electrolyte impermeability, which determines the open-circuit voltage of PCFCs, are presented. The correlation between the electrochemical performance and microstructure of PCFCs is also addressed.

2. Experimental

$Ba(Zr_{0.84}Y_{0.15}Cu_{0.01})O_{3-\delta}$ (BZYCu) powders were prepared by a conventional solid-state reaction method. The starting materials, $BaCO_3$ (99.9%, CERAC), ZrO_2 (99%, Junsei), Y_2O_3 (99.9%, High Purity Chemical), and CuO (99.9%, High Purity Chemical), were weighed according to their stoichiometric ratio and mixed via ball milling in ethanol for 24 h by using zirconia balls. After ball milling, the mixed powders were calcined to obtain single-phase BZYCu. For the determination of the optimum calcination temperature, BZYCu powders were calcined in air for 2 h at various temperatures between 1100 °C and 1300 °C. Phase analysis of the calcined powders was carried out by X-ray diffractometry (Cu Kα, X'Pert PRO, PANalytical, Netherlands). The calcined powders were ball milled again in order to attain fine and uniform powder characteristics. The shrinkage behavior as a function of increasing temperature, which was carried out to check the sinterability of the BZYCu powders as compared with that of pure BZY powders, was analyzed using a dilatometer (DIL 402C, NETZSCH, Germany).

For the fabrication of the anode substrate with nickel oxide (NiO, Sumitomo, Japan) and calcined BZYCu powder, we applied a liquid condensation process (LCP) to achieve granulation, a process that is known to be very effective for obtaining the desired anode microstructure [20]. Actually, because large amounts of water and phenolic resin are used in LCP, this granulation method may not be suitable for direct application to proton-conducting ceramics because most of these ceramics exhibit poor chemical stability against water vapor and carbon dioxide. However, in this study, because we employed a BZY-based electrolyte, which has relatively good chemical stability against water vapor and carbon dioxide [13], we were able to use LCP for the granulation of the NiO and BZYCu anode substrate powders. For the granulation via LCP, NiO, BZYCu, and phenolic resin (KNG100, Kolon Chemical, Korea) were mixed with zirconia balls for 20 h in ethanol. Phenolic resin was used as both a binder and a pore-forming agent. The mixed slurry was poured into the stirred water to make the granules. The weight ratio of the powder mixture in the slurry was NiO:BZYCu = 54:46, which was equivalent to the volume ratio of Ni:BZYCu = 40:60 after reduction. The phase analysis of the granules was carried out by X-ray diffractometry (Cu Kα, X'Pert PRO, PANalytical, Netherlands).

In order to check the electrical properties of the anode substrate, the LCP-fabricated NiO–BZYCu granules were uniaxially pressed into plate form under 30 MPa for 15 min at 80 °C and then sintered at 1500 °C for 3 h. The sintered NiO–BZYCu composite was then reduced under hydrogen atmosphere at 800 °C for 3 h. The electrical properties of the reduced composite (Ni:BZYCu = 40:60 vol%) were measured under a wet hydrogen atmosphere [$P(H_2O) = 2.3 \times 10^3$ Pa, saturated at 20 °C] in the temperature range of approximately 200–800 °C. Conductivity was measured by the DC four-point probe method using a current source meter (KE6220, Keithley, USA) and a digital multimeter (KE2000, Keithley, USA). The microstructure of the anode substrate before and after the reduction was characterized by scanning electron microscopy (FEI XL-30, Philips, Netherlands).

For the fabrication of the full cell, the uniaxially pressed NiO–BZYCu anode substrate, which had an area of 8×8 cm^2 and a thickness of 1 mm, was pre-sintered at 1000 °C in air to remove all organic components from the anode substrate. The thin BZYCu film was then deposited on the pre-sintered NiO–BZYCu plate via screen printing. The resulting sample was then sintered at 1500 °C for 3 h in air. The sintering temperature of anode/electrolyte bilayer was determined by comparing the shrinkage behavior of each NiO–BZYCu anode with BZYCu electrolyte using a dilatometer (DIL 402C, NETZSCH, Germany). The final configuration of the sintered anode/electrolyte bilayer plate was approximately 6×6 cm^2 in area and ~0.8 mm

thick, whereas the thickness of the sintered electrolyte layer was ~10 μm. The sintered anode/electrolyte substrate was then mechanically machined to $2 \times 2\ cm^2$ for full cell fabrication. For the cathode formation, a $La_{0.6}Sr_{0.4}Co_{0.2}Fe_{0.8}O_{3-\delta}$ (LSCF)–BZY cathode synthesized by the glycine—nitrate process (GNP) was coated on the dense electrolyte by screen printing an area $1 \times 1\ cm^2$ in size and then sintering at 1050 °C for 3 h in air. The overall processing flow for the full cell fabrication is shown in Fig. 1.

For the performance test of the anode-supported planer cell, a single-cell stack was constructed with a cell, sealing material, a metallic interconnect, and metal current collectors. A specially designed compression-seal gasket based on a glass/ceramic composite [21] was employed for sealing. A metallic interconnect based on a commercial alloy (Inconel 600, Nilaco, Japan) that is known to have good oxidation resistance was used. For better electrical contacts, a porous Ni sponge and a Pt mesh were used as current collectors for the anode side and the cathode side, respectively. Before the cell performance test, the single-cell stack was heated to 650 °C and then reduced in a hydrogen atmosphere. Cell conditioning was performed prior to the performance test in order to stabilize the interface between each cell component. Proper conditioning time was determined by checking the saturation of the cell voltage under constant current load conditions of −0.01 A.

After stable open-circuit voltage (OCV) was obtained, current–voltage and current–power characteristics were measured using air as the oxidant and moisturized hydrogen with 3% water (H_2+3% water) as the fuel at a fixed operating temperature. The open-circuit voltage and electrochemical impedance were measured with a Solartron 1287/1260 device and analyzed with the Z-VIEW commercial program. The frequency range for the AC impedance analysis was from 1×10^6 to 1×10^{-1} Hz.

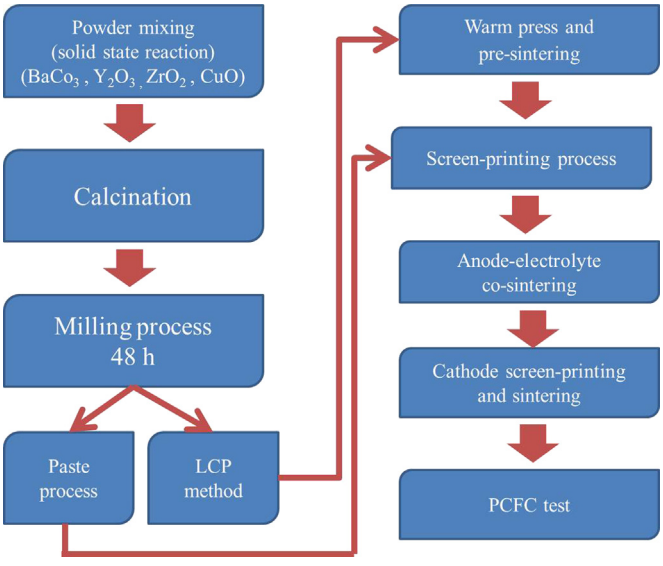

Fig. 1. Overall fabrication process of protonic ceramic fuel cells (PCFCs).

3. Results and discussion

3.1. Synthesis of BZYCu electrolyte powders

Fig. 2 shows the X-ray diffraction patterns of the BZYCu powder calcined at various temperatures between 1100 °C and 1300 °C. As shown in Fig. 2, the 1100 °C and 1200 °C calcinations were not sufficient to obtain single-phase BZYCu because a Y_2O_3 secondary phase was observed. Therefore, we adjusted the calcination temperature to 1300 °C to obtain single-phase BZYCu with a perovskite structure. In order to obtain fine powder characteristics to enhance the sinterability, the calcined powders were ball milled for 24 h and 48 h. According to the surface area analysis with BET, the specific surface areas gradually increased from 2.4 m^2/g to 7.1 and 12.2 m^2/g after ball-milling for 24 h and 48 h, respectively. Hence, we chose the BZYCu powder ball milled for 48 h as our standard condition. Fig. 3 shows the SEM micrograph of the BZYCu powder after calcination at 1300 °C and milling for 48 h; its final specifications were a mass-median diameter ($D50$) of 0.3 μm and a specific surface area of 12.2 m^2/g.

Fig. 4 shows the shrinkage behavior of 15 mol% Y-doped $BaZrO_3$ with and without the stoichiometric addition of 1.0 mol% CuO. It is obvious that the CuO addition enhanced the sinterability of the 15 mol% Y-doped $BaZrO_3$ even though the specific mechanism for enhanced sinterability is still not clear. At this moment, the significant increase in shrinkage as a result of CuO addition could be attributed to the liquid phase that formed during the sintering process [$T_{melting}$(CuO)= 1326 °C], which enhanced the matter transport through the liquid phase for the sintering.

3.2. Fabrication of single cells

Fig. 5 shows the X-ray diffraction patterns of the Ba$(Zr_{0.84}Y_{0.15}Cu_{0.01})O_{3-\delta}$ (BZYCu) powders and the NiO–BZYCu granules after LCP. As shown in the figure, the NiO–BZYCu granules have no secondary phase, indicating that the BZYCu was not decomposed during the LCP even though it was exposed to a water-containing solution.

Fig. 6 shows the dilatometric and thermogravimetric test results for the NiO—BZYCu granules made of LCP. In Fig. 6, the

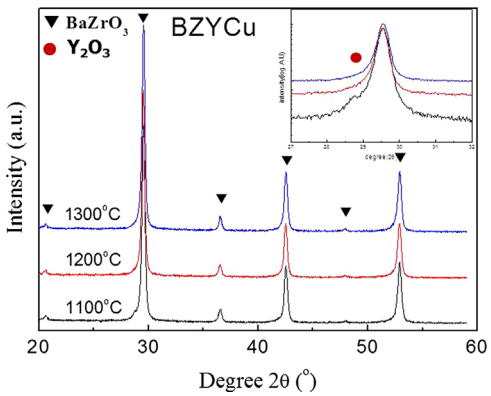

Fig. 2. X-ray diffraction patterns of the BZYCu powders after calcination.

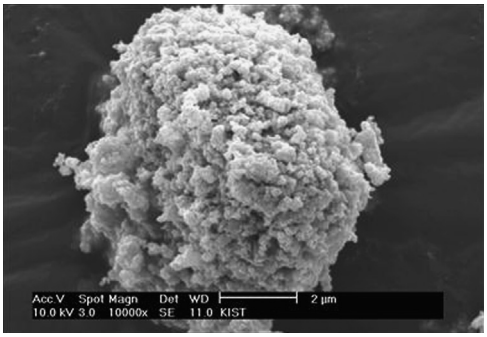

Fig. 3. SEM micrograph of powder after 1300 °C calcination and milling for 48 h.

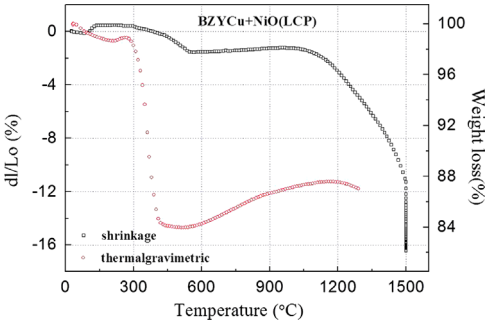

Fig. 6. Dilatometric and thermogravimetric test results for the BZYCu+NiO composite granule made with LCP.

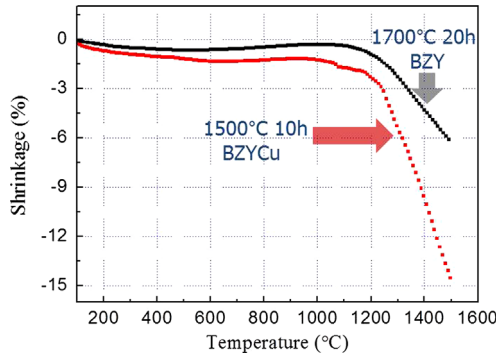

Fig. 4. Shrinkage behavior of 15 mol% Y-doped $BaZrO_3$ with and without the stoichiometric addition of 1.0 mol% CuO.

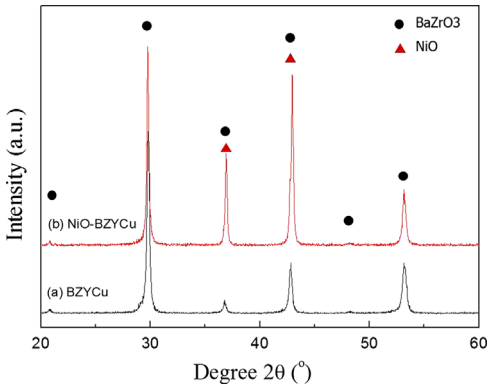

Fig. 5. X-ray diffraction patterns of BZYCu powder and NiO—BZYCu granule.

weight loss of 15 wt% up to 600 °C was mainly due to the burn-out of the phenolic resin, which was 25 wt% of the total weight. The initial shrinkage of NiO–BZYCu up to 600 °C, i.e., during the burnout of the phenolic resin, was 1.5% and the final shrinkage after sintering at 1500 °C was approximately 11%. The shrinkage further increased up to 17% after 2 h holding at 1500 °C, which was thought to be sufficient for the fabrication of PCFC anode substrates.

For the optimization of the anode microstructure, we examined the effect of uniaxial compaction pressure on the porosity and density of the NiO–BZYCu anode substrate. Fig. 7 shows the compaction pressure-dependence of the porosity and density of the NiO–BZYCu substrate after sintering at 1500 °C. As shown in Fig. 7, the density of the anode substrate monotonically increased as the compaction pressure increased. By considering the general criteria of anode porosity, we chose 30 MPa as an optimum compaction pressure for producing 30% porosity in the sintered NiO–BZYCu anode substrate, which would be equivalent to 43.4% porosity after reduction of the anode substrate. Fig. 8 shows the back-scattered electron (BSE) images of NiO–BZYCu and Ni–BZYCu. The black-, gray-, and white-colored regions represent the pores, BZYCu, and Ni, respectively. As shown in Fig. 8, the constituent components are finely and uniformly distributed, and the porosity of the anode substrate increased after reduction to the level where the fuel gas could flow sufficiently. The porosity increase in anode substrate was due to the formation of pores during the reduction of NiO to Ni.

Fig. 9 shows the conductivity of Ni–BZYCu, which shows that the electrical conductivity of Ni–BZYCu increased with decreasing temperature, which is typical metallic conduction behavior. This means that the use of 40 vol% Ni was sufficient to accomplish the percolation of Ni particles, enabling control over the overall conductivity. The conductivity of Ni–BZYCu at 600 °C was over 600 S/cm, which is sufficiently higher than the normally required 100 S/cm for PCFC anodes.

The electrolyte layer was coated onto the NiO–BZYCu anode substrate by screen printing. Before the screen printing, the anode substrate was pre-sintered to secure the strength of the anode substrate for the screen printing. The pre-sintering temperature was determined using the criteria of minimum shrinkage to allow for sufficient shrinkage during the co-sintering of the anode/electrolyte. Fig. 10 shows the dilatometric results for the anode substrate and the electrolyte bulk sample. As shown in the figure, the anode substrate and electrolyte begin to shrink at 1100 °C and 1200 °C, respectively. Thus, we adjusted the pre-sintering temperature of the anode substrate to 1000 °C, at which point the shrinkage was approximately 4%. Furthermore, because the electrolyte shrinkage rate is faster than that of the anode substrate, meaning they cross each other at around 1300 °C, we selected 1500 °C as the final temperature of the anode/electrolyte co-firing.

Fig. 11 shows the SEM images of the surface [Fig. 11(a), (b)] and cross section [Fig. 11(c)] of the anode/electrolyte

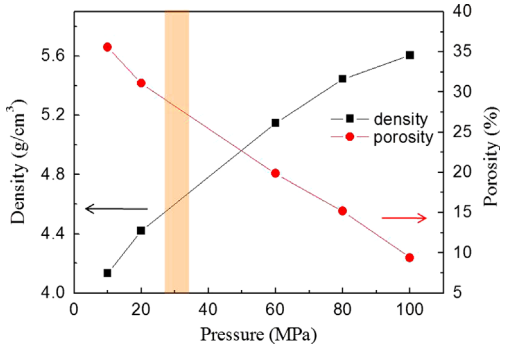

Fig. 7. Compaction pressure-dependence of the porosity and density of BZYCu+NiO substrate after sintering at 1500 °C.

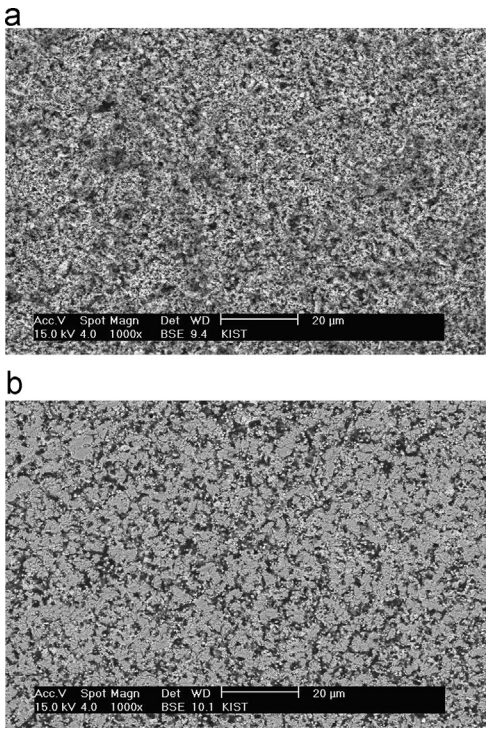

Fig. 8. Back-scattered electron (BSE) images of (a) NiO–BZYCu and (b) Ni–BZYCu.

bilayer after sintering at 1500 °C. As shown in the figure, small pores were observed on the electrolyte surface but they did not pierce through the electrolyte. It was found that the electrolyte was 10 μm in thickness and dense enough to block any gas leakage through the electrolyte. The LSCF–BZY cathode synthesized by GNP was coated on the dense electrolyte by screen printing. Fig. 12 shows the X-ray diffraction data of the LSCF–BZY cathode after sintering at 1050 °C for 3 h in air. As seen in Fig. 12, no secondary phase appeared in the LSCF–BZY cathode composite even after sintering.

3.3. Characterization of single cell performance

It is generally known that cell performance can be increased by current loading for a certain length of time during the initial

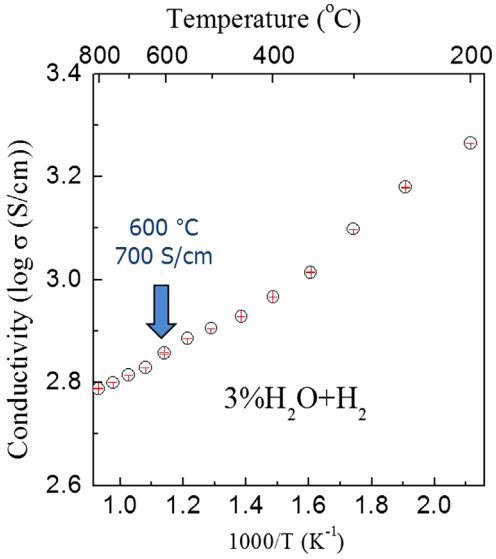

Fig. 9. Temperature-dependence of electrical conductivity of Ni—BZYCu.

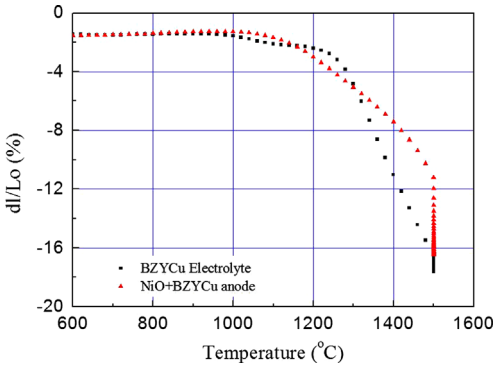

Fig. 10. Shrinkage behavior of anode substrate and electrolyte from dilatometric analysis.

operation period, which is called performance conditioning. Fig. 13 shows typical voltage variation behavior during conditioning. As shown in the figure, the voltage sharply increased in the first 2 h and was then saturated after 3 h. Accordingly, the OCV also increased from 0.95 to 0.985 after 3 h conditioning.

The electrochemical performance of the prepared cell also varied with respect to the conditioning time. As shown Fig. 14, the peak power density increased from 23 to 28.2 mW cm^{-2} at 650 °C after 3 h conditioning with −0.01 A. However, the cell performance was very poor due to the larger ohmic and polarization resistance of the cell which was confirmed from impedance spectroscopy results in Fig. 15. Nevertheless, the open-circuit voltage (OCV) was as high as 0.985 V at 650 °C which close to the theoretical one, indicating that the electrolyte membrane was sufficiently dense. This lower performance of a single cell, as shown in Fig. 14, can be attributed to various structural imperfections in the cell components: (1) cracks or pinholes in the electrolyte layer, (2) delamination of the electrode from the electrolyte, and (3) nonoptimized cell structure, especially in the cell components related to electrochemical activity

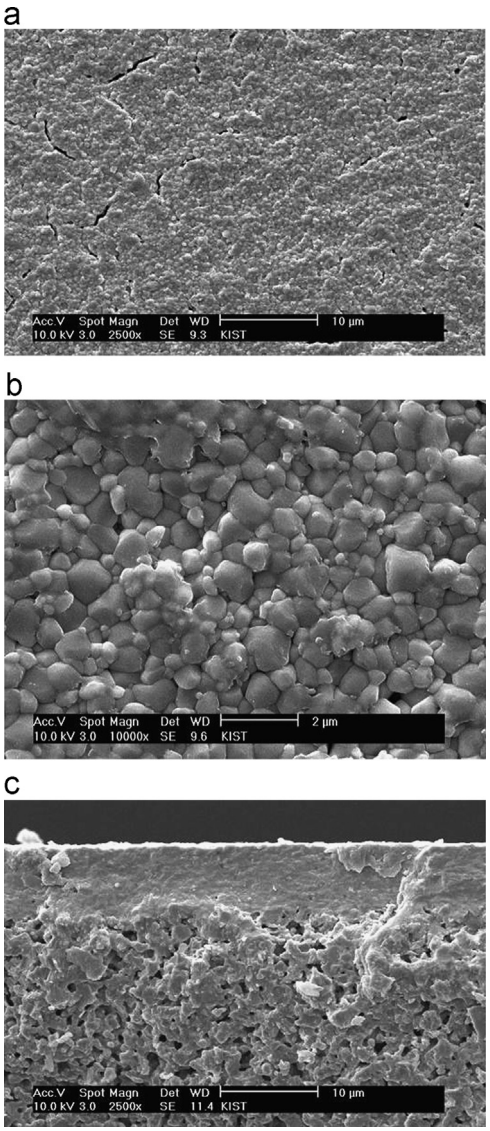

Fig. 11. SEM image of anode—electrolyte bilayer after sintering at 1500 °C: (a) surface, (b) surface-high magnification and (c) cross section.

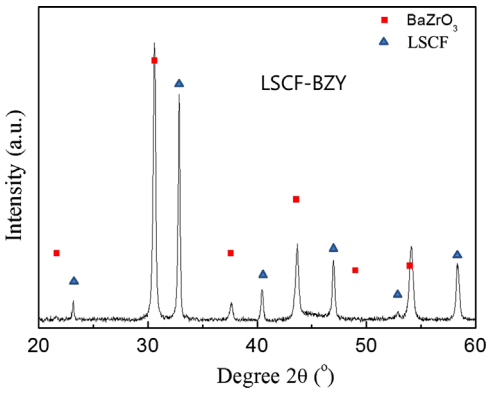

Fig. 12. X-ray diffraction pattern of LSCF—BZY cathode after sintering at 1050 °C for 3 h in air.

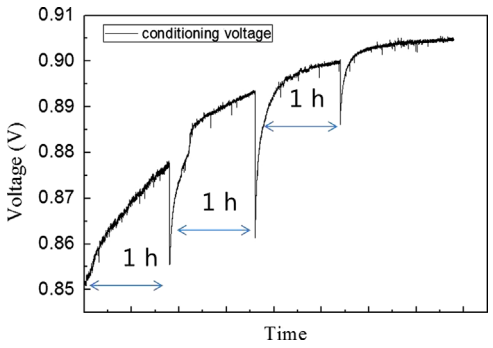

Fig. 13. Typical temporal variation of cell voltage during conditioning.

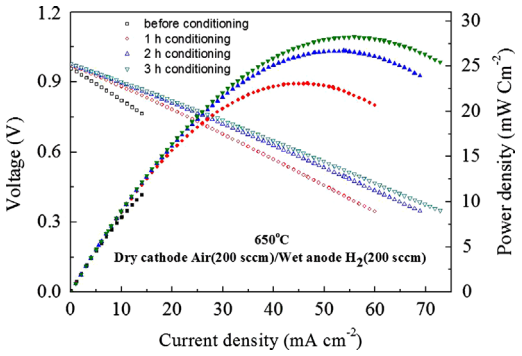

Fig. 14. *I*—*V* characteristics (open symbols) and power density curves (closed symbols) before and after conditioning.

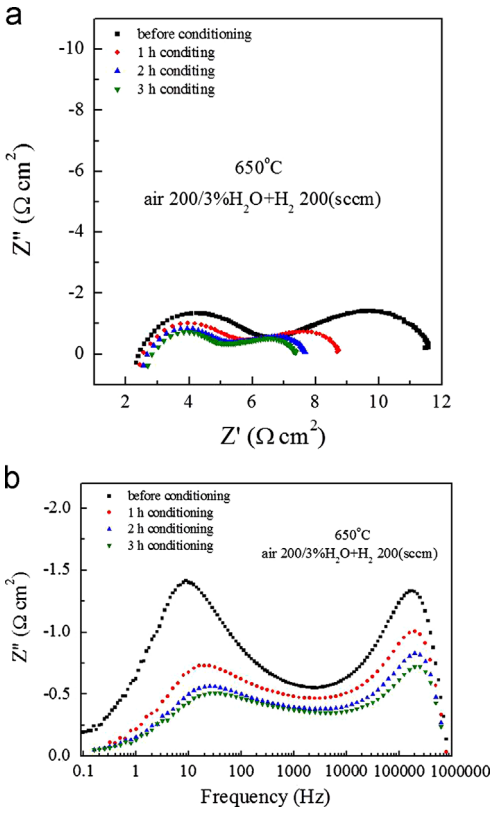

Fig. 15. (a) Nyquist and (b) Bode plots of the single cell measured under open-circuit and current load (−0.01 A) for conditioning.

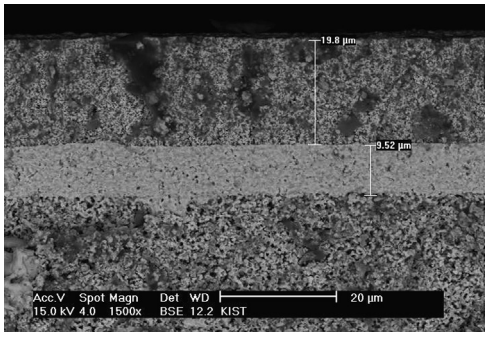

Fig. 16. Post-mortem analysis of the cell. Cross-sectional view of NiO—B-ZYCu/BZYCu (10 μm)/LSCF–BZY(25 μm).

and current-collecting efficiency. However, as shown in the cross-sectional view (Fig. 13) from the post-mortem analysis on the cell, the BZYCu electrolyte maintained a very dense structure, and it adhered well with the neighboring anode and cathode layers. From these results, the main cause of lower cell performance can be attributed to the nonoptimized cell structure. As shown in Fig. 16, we did not employ an anode functional layer on the anode side, which is essential for minimizing the anode over-potential. Furthermore, we used only LSCF–BZY composite materials for the cathode, which might have deteriorated the current-collecting efficiency on the cathode side. Either or both problems in anode and cathode structures should be solved for the improvement of cell performance.

4. Conclusions

A thin and dense $Ba(Zr_{0.84}Y_{0.15}Cu_{0.01})O_{3-\delta}$ (BZYCu) electrolyte was successfully fabricated on a porous anode substrate at a relatively low sintering temperature of 1500 °C by using an enhanced sintering method with 1 mol% of CuO as a sintering additive. From the dilatometric analysis, the optimum co-sintering conditions of electrolyte/anode was determined by matching the shrinkage of the BZYCu electrolyte and the porous NiO–BZYCu anode composites, resulting in the formation of a dense and thin electrolyte layer with a thickness of 10 μm. From the electrochemical characterization of the PCFC at 650 °C, we found that the electrolyte membrane was sufficiently dense to produce close to the theoretical open-circuit voltage (OCV) of 0.98 V at 650 °C. However, the electrochemical performance of the anode-supported PCFCs remained low due to the nonoptimized electrode microstructure, especially in terms of the electrochemical activity of the anode and the current-collecting efficiency of the cathode. Hence, further improvements in the electrode microstructure are necessary in order to enhance the electrochemical performance of BZYCu-based PCFCs, which will be reported in our forthcoming paper.

Acknowledgment

This research was supported by **the Fusion Research Program for Green Technologies** through the National Research Foundation of Korea (NRF), funded by the Ministry of Education, Science and Technology (2011–0019297) and in part by the Institutional Research Program of the Korea Institute of Science and Technology (KIST).

References

[1] N. Minh, Ceramic fuel cells, Journal of the American Ceramic Society 76 (3) (1993) 563–588.
[2] B. Steele, A. Heinzel, Materials for fuel-cell technologies, Nature 414 (6861) (2001) 345–352.
[3] E. Ivers-Tiffée, A. Weber, D. Herbstritt, Materials and technologies for SOFC-components, Journal of the European Ceramic Society 21 (10–11) (2001) 1805–1811.
[4] V.V. Kharton, et al., Ceria-based materials for solid oxide fuel cells, Journal of Materials Science 36 (5) (2001) 1105–1117.
[5] J. Fergus, Electrolytes for solid oxide fuel cells, Journal of Power Sources 162 (1) (2006) 30–40.
[6] T. Yamada, et al., Development of intermediate-temperature SOFC module using doped lanthanum gallate, Journal of the Electrochemical Society 151 (10) (2004) A1712–A1714.
[7] H. Iwahara, High-Temperature proton conducting oxides and their applications to solid electrolyte fuel-cells and steam electrolyzer for hydrogen-production, Solid State Ionics 28 (1988) 573–578.
[8] K.D. Kreuer, et al., Transport in proton conductors for fuel-cell applications: simulations, elementary reactions, and phenomenology, Chemical Reviews 104 (10) (2004) 4637–4678.
[9] K.H. Ryu, S.M. Haile, Chemical stability and proton conductivity of doped $BaCeO_3$–$BaZrO_3$ solid solutions, Solid State Ionics 125 (1–4) (1999) 355–367.
[10] H. Iwahara, Proton conducting ceramics and their applications, Solid State Ionics 86–88 (1996) 9–15.
[11] T. Norby, Solid-state protonic conductors: principles, properties, progress and prospects, Solid State Ionics 125 (1–4) (1999) 1–11.
[12] K.D. Kreuer, Proton-conducting oxides, Annual Review of Materials Research 33 (2003) 333–359.
[13] P. Babilo, S.M. Haile, Enhanced sintering of yttrium-doped barium zirconate by addition of ZnO, Journal of the American Ceramic Society 88 (9) (2005) 2362–2368.
[14] K.D. Kreuer, et al., Proton conducting alkaline earth zirconates and titanates for high-drain electrochemical applications. in: Proceedings of High Temperature Materials Chemistry, Pts I and II, 2000, 15, pp. 735–740.
[15] J.S. Park, et al., Low temperature sintering of $BaZrO_3$-based proton conductors for intermediate temperature solid oxide fuel cells, Solid State Ionics 181 (3–4) (2010) 163–167.
[16] D.Y. Gao, R.S. Guo, Structural and electrochemical properties of yttrium-doped barium zirconate by addition of CuO, Journal of Alloys and Compounds 493 (1–2) (2010) 288–293.
[17] E.O. Oh, et al., Extremely thin bilayer electrolyte for solid oxide fuel cells (SOFCs) fabricated by chemical solution deposition (CSD), Advanced Materials 24 (25) (2012) 3373–3377.
[18] G.J. Wright, J.A. Yeomans, Constrained sintering of yttria-stabilized zirconia electrolytes: the influence of two-step sintering profiles on microstructure and gas permeance, International Journal of Applied Ceramic Technology 5 (6) (2008) 589–596.
[19] S. Kwon, G.L. Messing, Constrained densification in boehmite–alumina mixtures for the fabrication of porous alumina ceramics, Journal of Materials Science 33 (4) (1998) 913–921.
[20] J.H. Lee, et al., The impact of anode microstructure on the power generating characteristics of SOFC, Solid State Ionics 158 (3–4) (2003) 225–232.
[21] J.H. Lee, et al., Effect of elastic network of ceramic fillers on thermal cycle stability of a solid oxide fuel cell stack, Advanced Energy Materials 2 (4) (2012) 461–468.